Jose Julio Gutiérrez, Izaskun Azcarate, Puri Saiz, Andoni Lazkano, Luís Alberto Leturiondo, Koldo Redondo, “An alternative strategy to improve the flicker severity measurement”, International Journal of Electrical Power and Energy Systems, Volume 63, 2014, Pages 667-673, ISSN 0142-0615, https://doi.org/10.1016/j.ijepes.2014.06.059

(https://www.sciencedirect.com/science/article/pii/S0142061514004177)

Abstract: The IEC 61000-4-15 standard defines a flickermeter that is universally accepted as the meter used for the objective measurement of a disturbing light flicker. The accurate results provided by the IEC flickermeter under uniform fluctuations stand in contrast with its unpredictable behavior under real conditions when voltage fluctuations are not uniform over time. Under nonuniform fluctuations, the IEC flickermeter can indicate wrong values, and this could explain the absence of users’ complaints at sites where high flicker levels were measured. This work presents a new strategy for flicker measurement that overcomes the deficiencies presented in the IEC flickermeter, properly relating flicker severity values and temporal evolution of the fluctuation. The manuscript describes in detail the functional and design specifications of the new strategy, as well as the results obtained during the validation process in which the IEC flickermeter and the new strategy were subjected to input signals with different temporal fluctuation patterns. The manuscript also presents a comparison between the response of the two strategies to real voltage signals, which are complex and nonuniform in nature. The results confirm the differences between both strategies, despite both meet the same requirements established by the standard.

Keywords: Power quality, flicker, nonuniform voltage fluctuations, flickermeter.

An Alternative Strategy to Improve the Flicker Severity Measurement

J.J. Gutierrez[a], I. Azcarate[*,a], P. Saiz[a], A. Lazkano[a], L.A. Leturiondo[a], K. Redondo[a]

Affiliation and adresses:

[a] Communications Engineering Department.

University of the Basque Country UPV/EHU.

Alameda Urquijo S/N

48013 Bilbao, Spain

Corresponding author:

[*] I. Azcarate

email: izaskun.azkarate@ehu.es

Tel. : +34946018209

Fax. : +34946014259

Abstract

The IEC 61000-4-15 standard defines a flickermeter that is universally accepted as the meter used for the objective measurement of a disturbing light flicker. The accurate results provided by the IEC flickermeter under uniform fluctuations stand in contrast with its unpredictable behavior under real conditions when voltage fluctuations are not uniform over time. Under nonuniform fluctuations, the IEC flickermeter can indicate wrong values, and this could explain the absence of users' complaints at sites where high flicker levels were measured. This work presents a new strategy for flicker measurement that overcomes the deficiencies presented in the IEC flickermeter, properly relating flicker severity values and temporal evolution of the fluctuation. The manuscript describes in detail the functional and design specifications of the new strategy, as well as the results obtained during the validation process in which the IEC flickermeter and the new strategy were subjected to input signals with different temporal fluctuation patterns. The manuscript also presents a comparison between the response of the two strategies to real voltage signals, which are complex and nonuniform in nature. The results confirm the differences between both strategies, despite both meet the same requirements established by the standard.

Keywords

Power quality, flicker, nonuniform voltage fluctuations, flickermeter.

1. Introduction

The supply voltage may vary under changes in load conditions or in the operation of the generation systems, and these variations produce flicker of the lighting equipment. Flicker is understood as the disturbing sensation that is experienced by the human visual system when subjected to these light fluctuations, leading to potential complaints. A flickermeter must objectively quantify the discomfort produced by a reference light source when its supply voltage fluctuates, in order to reduce the expense of corrective measures for both the owner of the disturbing equipment and the electrical company. Thus, the effective calculation of flicker severity becomes essential in the monitoring performed by the metering equipment [1].

The universally accepted flicker measurement method was developed by the International Union for Electricity Applications (UIE) during the 1980s [2] and was first published as the standard IEC 868 in 1992. This standard established the functional and design specifications for the International Electrotechnical Commission (IEC) flickermeter and defined short-term flicker severity, P_{st}, as the fundamental parameter used to evaluate the discomfort. Afterwards, the specification was classified as the IEC 61000-4-15 standard, and its last edition was published in 2010 [3] with the objective of a greater convergence in the results provided by different commercial implementations. During the last 10 years, the unpredictable behavior of the IEC flickermeter under real conditions has put its accuracy in assessing the perceived flicker severity under question [4, 5]. The main argument in clarifying this issue points to the extensive use of efficient lighting technologies that are less sensitive to flicker than the incandescent one that is used as the reference lamp in the current standard [5, 6]. There is also a concern about the idea that the IEC flickermeter needs improvement when dealing with interharmonics that cause flicker [7]. However, according to the findings presented in [8], the most convincing explanation for the poor behavior of the IEC flickermeter in real scenarios comes from the inherent deficiencies in its specification. The response of the IEC flickermeter is not correct when the fluctuations are not uniform over time. The design of its complex specification did not particularly consider the dependence of flicker severity on temporal evolution of the fluctuation. In fact, the final specification was adjusted for a set of uniform rectangular fluctuations, a simple model of the fluctuations in real scenarios. However, the nonuniform characteristics of the real fluctuations in some locations lead the IEC flickermeter to provide wrong values. In these cases, the assessed flicker severity differs from the actual perception of the users, explaining the poor correlation with their complaints [8].

The current work presents a new strategy for measuring flicker severity. This strategy provides an alternative to the IEC flickermeter as it suggests a method that properly correlates flicker severity and temporal evolution of the fluctuation, complying with the accuracy requirements of the IEC 61000-4-15 standard. The work describes the new strategy and sets out the reasons for its success in evaluating the flicker severity produced by nonuniform fluctuations. The new strategy is described as a simple outline that can be easily adapted from the current configuration specified by the IEC 61000-4-15 standard. The work provides all the details required for the design and the implementation of the new strategy. Finally, the work presents a comparison between the two strategies when subjected to analytical input signals both with uniform and nonuniform temporal fluctuation patterns. Moreover, the work shows the different behavior of the two strategies with real voltage signals, due to the complexity and irregularity of their fluctuations.

2. Description of the IEC flickermeter

Fig. 1 shows the block diagram of a flickermeter according to the specification defined in IEC 61000-4-15. In Block 1, the input voltage $u(t)$ is scaled to an internal reference value to make flicker measurements independent of the input voltage level.

In Block 2, the scaled input voltage $u_1(t)$ is demodulated by means of a squaring multiplier, thereby simulating the behavior of an incandescent lamp.

Block 3 comprises three cascaded filters. The first two filters complete the demodulation process and consist of a 1$^{\text{st}}$-order high-pass filter (3 dB cutoff frequency $f_{\text{co}} = 0.05$ Hz) and a 6$^{\text{th}}$-order low-pass Butterworth filter (3 dB cutoff frequency $f_{\text{co},50} = 35$ Hz for 50 Hz systems). The third filter is a band-pass filter that models the behavior of the lamp–eye system. Its design was defined from experiments carried out by H. de Lange and P. Ailleret in the 1950s [9, 10] and its transfer function is given in the standard [3]. The output of Block 3 is $u_3(t)$, which represents the weighted demodulated voltage-change signal.

Block 4 of the flickermeter implements the *eye–brain* model proposed by Rashbass and Koenderink [11, 12]. This block includes a squaring multiplier that simulates the nonlinear eye–brain response, followed by a low-pass filter that accounts for the perceptual storage effects in the brain. The low-pass filter is specified to be a sliding mean filter with a time constant of 300 ms. The filtered signal is then multiplied by a scaling factor to obtain

P_{inst}. The unit of P_{inst} corresponds to the reference human flicker perceptibility threshold, experimentally obtained through subjective tests [2].

Block 5 evaluates the flicker severity by applying a multipoint algorithm that uses the percentiles obtained from the cumulative probability function (CPF) over a short period (usually 10 min) of P_{inst}. The adjustment of the algorithm was carried out by using the experimental curve of the flicker severity threshold, $P_{\text{st}} = 1$ [13], obtained for different frequencies of rectangular voltage fluctuations. Once the values of the coefficients and percentiles were calculated, all the points of the curve for $P_{\text{st}} = 1$ fitted with errors under 5%. Initially, the selected percentiles were $P_{0.1}$, P_1, P_3, P_{10} and P_{50}. Later, some of these were substituted by other smoothed percentiles, P_{1s}, P_{3s}, P_{10s} and P_{50s}, each of them obtained from a set of *unsmoothed* percentiles. Consequently, the standard [3] obtains a flicker severity value from a total of 15 *unsmoothed* percentiles as:

$$P_{st} = \sqrt{0.0314 \cdot P_{0.1} + 0.0525 \cdot P_{1s} + 0.0657 \cdot P_{3s} + 0.28 \cdot P_{10s} + 0.08 \cdot P_{50s}} \qquad (1)$$

3. Deficiencies of the IEC flickermeter

The evolution of the IEC 61000-4-15 standard has been aimed at increasing the accuracy of flicker measurement. The most significant progression corresponds to the 2.0 edition, which includes a new set of functional tests in order to restrict the implementation margins. This improvement has contributed to the convergence of the results from the commercial implementations under the same input conditions [14]. However, during the last years, several studies have warned about the unpredictable behavior of the IEC flickermeter under real conditions [15, 16]. Additionally, in many networks that supply industrial areas, the real flicker severity values are much higher than the planning levels without causing complaints by residential customers. However, other loads that generate flicker that is clearly over the planning levels, but quite close to the former cases, lead to complaints by customers, requiring corrective actions [4, 5]. In fact, different working groups created for the improvement of the electric power system have studied the possibility of modifying the IEC 61000-4-15 standard to solve those problems. On the one hand, the working group C4.108 of CIGRE

(International Council on Large Electric Systems) specifically states that a major objective of its final report is ... *to present methods and techniques which could result in improved correlation* ... [5]. On the other hand, the working group C4.111 of CIGRE has established as a part of its scope ... *to recommend possible alternatives to the flickermeter concept of* P_{st} *for specifying, measuring, and assessing voltage fluctuations...* [17].

There is a general opinion that the discrepancies are mainly because the IEC flickermeter design took the incandescent lamp as the reference lamp, whereas today there are new lighting technologies on the market that are less sensitive to flicker. Consequently, some authors suggest the adaptation of the IEC flickermeter to the modern lamps [5]. Nevertheless, the latter lighting technologies cannot be considered as stable or fully evolved. Even assuming their low sensitivity characteristics, these lamps presented a low market penetration rate at the time when the aforementioned studies were carried out [18], and thus the use of these new lamps would not explain the absence of complaints.

On the other hand, some of those works consider the planning levels as excessively cautious and conservative, advising the regulatory institutions to raise the planning levels clearly above the current limits. Such actions would obviously save on corrective costs, but at the same time, they would be unfavorable for users in locations where the flicker measurement and the complaints were correlated.

Once the extrinsic explanations have been considered, it seems necessary to review whether the way in which the IEC flickermeter performs the measurement is consistent with the way in which people perceive irritation. This approach leads to examining possible causes of discrepancies related to the built-in features of the IEC flickermeter specification. On the one hand, initially the multipoint algorithm used five percentiles for the calculation of the flicker severity. However, the validation process of the algorithm warned about its inconsistency under irregular fluctuations in real circumstances. The solution was to increment the number of percentiles involved in the algorithm [2]. On the other hand, a recent work presents an exhaustive analytical study of the improper behavior of the IEC flickermeter under nonuniform temporal fluctuation patterns, more representative of real scenarios [8]. Moreover, the study confirms the deviations by means of several subjective experiments using voltage signals recorded in real locations affected by relevant values of flicker. The main conclusions of the work warn about the increasing malfunction of the IEC flickermeter as the irritation becomes less uniform along the integration period.

To understand fully this anomalous behavior, knowledge of how the irritation is related to the amplitude and time distribution of the light fluctuation is required. P. Ailleret established these associations in the 1950s [10] by means of different physiological experiments. On the one hand, that study established that the irritation depends linearly on the amplitude; that is, should the amplitude double, the irritation must also double. In fact, this characteristic is a specific requirement of the standard IEC 61000-4-15 [3]. On the other hand, the irritation is nonlinearly related to the product of the square of the amplitude, A, and the duration, T, of the fluctuation:

$$Irritation = f\left(A^2 \cdot T\right) \ . \tag{2}$$

For example, a regular fluctuation of amplitude A during the whole integration period (10 min) generates the same effect as one that fluctuates during $\frac{1}{4}$ of the integration period with $2A$ amplitude and does not fluctuate during $\frac{3}{4}$ of the integration period. Nevertheless, the IEC flickermeter was not conceived considering this requirement; the specification of Block 5, which is finally responsible for the flicker severity measurement, was designed for a set of rectangular voltage fluctuations. According to [8], the statistical strategy specified in Block 5 works properly for regular fluctuations but generates relevant deviations when the fluctuation pattern is not uniform over time.

The conclusions of the work [8] and the Block 5 definition process itself confirm the need for a new strategy for flicker measurement that should properly consider the compliance with the time composition rule established by P. Ailleret. However, any alternative solution should not be adapted for a specific set of fluctuations but should be a universal strategy valid for any type of nonuniform fluctuations in complex and real scenarios.

4. An alternative strategy for the flicker severity measurement

The multipoint algorithm of Block 5 does not properly assess the flicker severity generated by fluctuations that are not uniform over time. An initial approach to solving this problem could be to replace the current Block 5 with another one that functions properly in the presence of nonuniform fluctuations. The new strategy should be based on an average estimator, compliant with Ailleret's rule relating amplitude and duration (2) but preserving the physical properties and dimensions of the flicker severity modeled by [9–12].

A possible parameter for that purpose would be the square root of the mean value of P_{inst}. This is a simplified version of the multipoint algorithm. If the smoothing effect of the low-pass filter of Block 4 is dismissed, that parameter corresponds to the root mean square of the output of Block 3, $u_3(t)$:

$$V_{\text{rms,b3}} = \sqrt{\frac{1}{T_0} \int_{T_0} u_3^2(t) dt} \ , \tag{3}$$

where T_0 corresponds to the short-time integration period.

To evaluate the effect of this primary strategy on the flicker severity measurement, the values of $V_{\text{rms,b3}}$ for rectangular voltage fluctuations of frequencies, f_{m}, up to 33.3 Hz (4000 changes per minute or cpm) and relative amplitudes, $\frac{\Delta V}{V}$, corresponding to $P_{\text{st}} = 1$, were calculated. The values were within the accuracy required by IEC 61000-4-15 for the flicker severity measurement, namely 1 ± 0.05, for fluctuation frequencies from approximately 7 Hz (840 cpm) to 33.3 Hz. However, for frequencies below 7 Hz, the results from the $V_{\text{rms,b3}}$ estimator decrease with fluctuation frequency, diverging from the required accuracy. The underlying impression of this preliminary study is that the $V_{\text{rms,b3}}$ estimator could be a proper method for assessing the flicker severity. Nevertheless, the strategy requires an intermediate linear system to adjust the results of the root mean square (RMS) calculation to the 1 ± 0.05 accuracy range for frequencies below 7 Hz.

Based on these assumptions, Fig. 1 shows the functional block diagram of the alternative strategy for flicker severity measurement. The block diagram follows the physiological lamp–

eye–brain model exactly as it is defined by the IEC 61000-4-15 standard, maintaining the instantaneous flicker perception, P_{inst}. Additionally, the output of Block 3 is weighted by a new linear system aimed at measuring flicker severity by means of the RMS calculation. Considering the linear relation between flicker severity and the amplitude of the fluctuation, the RMS value of a nonuniform fluctuation, $s_{\mathrm{nu}}(t)$, consisting of a single regular fluctuation $s_1(t)$, applied during a time t_1, followed by another regular fluctuation $s_2(t)$, applied during a time t_2, complies with Ailleret's rule relating irritation and time (2), by the expression:

$$V_{rms,s_{nu}} = \sqrt{\tfrac{V_1^2 t_1 + V_2^2 t_2}{t_1 + t_2}}\ , \tag{4}$$

where V_1 and V_2 are the RMS values of the single regular fluctuations, $s_1(t)$ and $s_2(t)$, respectively.

The general philosophy of the new strategy can be summarized as follows:

- It complies with the instantaneous flicker sensation, according to the flicker perceptibility threshold curve, experimentally obtained through subjective tests [2].

- It is conceived to assess the flicker severity having the experimental flicker severity curve, $P_{\mathrm{st}} = 1$, as the reference [2, 13].

- It maintains the linear relation between flicker severity and the relative amplitude of the fluctuation, as it is currently specified in the IEC 61000-4-15 standard [3]. The output of the new linear system is proportional to the relative amplitude $\frac{\Delta V}{V}$; therefore, its RMS value is too.

- The combination of the new linear system and the RMS estimator allows compliance with Ailleret's rule (2) relating irritation and time [10].

The challenge involves the design of a new linear system to validate the alternative strategy, confirming compliance with the previous conditions. The starting point must be based on the experimental $P_{\mathrm{st}} = 1$ curve, as it was in the case of the multipoint algorithm, to agree fully with specifications of the current standard.

4.1. Design of a new linear system

Following the procedure detailed in Fig. 1, the new linear system must be designed to weigh the output of Block 3 producing a unity RMS value for the rectangular voltage fluctuations of frequencies up to 33.3 Hz (4000 cpm) and amplitudes corresponding to the $P_{\mathrm{st}} = 1$ curve. Thus, the new linear system should be characterized by two fluctuation frequency ranges:

– $f_m \geq 7$ Hz (840 cpm): the new linear system must not modify the output of Block 3.

– $f_m < 7$ Hz: the module of the frequency response of the new linear system must weigh the output of Block 3 to obtain RMS values of 1 ± 0.05 for all the frequencies.

The specification of the frequency response module of the new filter, $H_{\mathrm{n,spec}}(f)$, requires the analytical characterization of the spectral content of the signals involved in the procedure. The flickermeter input signal, $u(t)$, can be expressed as follows:

$$u(t) = \sqrt{2}A\big(1 + g_{\mathrm{m}}(t)\big)\cos(\omega_o t) \ , \tag{5}$$

where $g_{\mathrm{m}}(t)$ corresponds to the rectangular voltage fluctuation with frequency f_{m} and relative amplitude $\frac{\Delta V}{V}$, modulating a sinusoidal carrier with frequency $\omega_o = 2\pi f_o$ and RMS value A.

After scaling the input amplitude to the reference value, A_{R}, and the subsequent quadratic demodulation, the output of Block 2 comprises the following terms:

$$u_2(t) = A_{\mathrm{R}}^2\left[\big(1 + \tfrac{1}{4}(\tfrac{\Delta V}{V})^2\big)\big(1 + \cos(2\omega_o t)\big) + 2g_{\mathrm{m}}(t)\big(1 + \cos(2\omega_o t)\big)\right]. \tag{6}$$

The rectangular voltage fluctuation can be expressed by the cosine-Fourier representation:

$$g_{\mathrm{m}}(t) = \sum_{n=0}^{\infty} a_n \cos(n\omega_{\mathrm{m}} t) \qquad a_n = \tfrac{\Delta V}{V}\tfrac{2}{n\pi}\sin\left(\tfrac{n\pi}{2}\right) \ , \tag{7}$$

characterizing the output of Block 2 as:

$$\begin{aligned} u_2(t) = A_{\mathrm{R}}^2 \Bigg[& \overbrace{2\sum_{n_1=0}^{\infty} a_{n_1} \cos(n_1\omega_{\mathrm{m}} t)}^{\text{present at the output of Block 3}} + \overbrace{\sum_{n_2=0}^{\infty} a_{n_2} \cos\big((n_2\omega_{\mathrm{m}} - 2\omega_o)t\big)}^{\text{present at the output of Block 3}} + \\ & + \overbrace{\Big(1+\tfrac{1}{4}(\tfrac{\Delta V}{V})^2\Big)\Big(1+\cos(2\omega_o t)\Big)}^{\text{dismissed by the filters of Block 3}} + \overbrace{\sum_{n_3=0}^{\infty} a_{n_3} \cos\big((n_3\omega_{\mathrm{m}} + 2\omega_o)t\big)}^{\text{dismissed by the filters of Block 3}} \Bigg] . \end{aligned} \tag{8}$$

The third and fourth terms consist of a DC component, as well as others above the $2f_o$ component that are strongly attenuated by the filters of Block 3, so they can be dismissed. The first two terms do affect the spectral composition of the input of the new linear system and, as a consequence, the measurement of flicker severity as well. Therefore, the output of Block 3 can be expressed as follows:

$$u_3(t) \approx A_{\mathrm{R}}^2 \left[2\sum_{n_1=0}^{\infty} b_{n_1} \cos(n_1\omega_{\mathrm{m}} t + \varphi_1) + \sum_{n_2=0}^{\infty} b_{n_2} \cos\big((n_2\omega_{\mathrm{m}} - 2\omega_o)t + \varphi_2\big) \right] , \tag{9}$$

where (b_{n_1}, b_{n_2}) and (φ_1, φ_2) are the amplitudes and angles, respectively, of $u_2(t)$ after being filtered by Block 3.

The numerical definition of the frequency specification of the new filter concerning the amplitude is based on the spectral composition of $u_3(t)$, according to (9). The method consists of the calculation of the desired value for each fluctuation frequency, starting from 840 cpm and iteratively descending to 1 cpm, so that the RMS value of the output of the new filter, $u_{4n}(t)$ is 1. From (9), the output of Block 4N of Fig. 1 can be expressed as:

$$\begin{aligned} u_{4n}(t) = & \overbrace{2A_{\mathrm{R}}^2 \sum_{n_1=0}^{\infty} |H_{\mathrm{n,spec}}(n_1\omega_{\mathrm{m}})| \cdot b_{n_1} \cos(n_1\omega_{\mathrm{m}} t + \varphi_1)}^{\text{Part A}} + \\ & + \overbrace{A_{\mathrm{R}}^2 \sum_{n_2=0}^{\infty} |H_{\mathrm{n,spec}}(n_2\omega_{\mathrm{m}} - 2\omega_o)| \cdot b_{n_2} \cos\big((n_2\omega_{\mathrm{m}} - 2\omega_o)t + \varphi_2\big)}^{\text{Part B}} , \end{aligned} \tag{10}$$

where for reasons of simplifying the method, the effect of the angle of the new filter has not been considered.

To address the resolution, several restrictions need to be established that limit the extension of (10). Considering the large attenuation introduced by the filters of Block 3 at frequencies above 35 Hz, the method uses components only up to 120 Hz. Even so, the process is still complex, and some additional restrictions need to be set. Part A of (10) contributes spectral components larger than or equal to f_{m}. Among these, those above 840 cpm are only affected by the values of the filters of Block 3, as the corresponding values of the new filter are established as 1. On the other hand, the components between f_{m} and 840 cpm are affected by the filters of Block 3 and, later on, also by the values of the new system, which are already known at the current iteration. Nevertheless, Part B of (10) may contribute components either above or below f_{m}. If they are above f_{m}, the guideline is the same as in Part A. Otherwise, if they are below f_{m}, the corresponding values of the new system are not available yet. To make the process solvable, the problem needs to be delimited further without compromising accuracy. The order n_2 of all the components of Part B below f_{m} is higher than 9 for f_{m} under 1200 cpm. As a consequence, the Fourier coefficients b_{n_2} are negligible, and those components can be disregarded.

The iterative method can be developed by consecutive resolution of an equation of a single unknown quantity, by applying the design criterion of the new flicker measurement strategy, i.e., the RMS value of $u_{4n}(t)$ must be 1. Starting at f_{m}=840 cpm, the values of $|H_{\mathrm{n,spec}}(f)|$ for the spectral components different from 840 cpm that are involved in (10) are known, $|H_{\mathrm{n,spec}}(f \neq f_{\mathrm{m}})|$=1 and the only unknown corresponding to $|H_{\mathrm{n,spec}}(f_{\mathrm{m}})|$. The same process is done again for the next modulation frequency, f_{m}=839 cpm. In this case, the values of $|H_{\mathrm{n,spec}}(f)|$ for all the spectral components above f_{m} are previously known, since $|H_{\mathrm{n,spec}}(f > f_{\mathrm{m}} + 1)|$=1 and the value of $|H_{\mathrm{n,spec}}(f_{\mathrm{m}} + 1)|$ has been obtained in the previous iteration. The process is repeated for all the f_{m} frequencies down to 1 cpm.

Finally, this specification needs to be characterized analytically by an approximation, $H_{\mathrm{n,appx}}(s)$, with a feasible implementation, like the following:

$$H_{\mathrm{n,appx}}(s) = k_n \frac{(s+\omega_{1n}) \cdot (s+\omega_{3n})}{(s+\omega_{2n}) \cdot (s+\omega_{4n})} \ . \tag{11}$$

The values of (11) are adjusted to minimize the root mean squared error of $|H_{\mathrm{n,appx}}(f)|$ in relation to the specification, $|H_{\mathrm{n,spec}}(f)|$. Thus, the final values for the parameters of $H_{\mathrm{n,appx}}(s)$ are as follows, taking into account that this transfer function is the one obtained for 230 V/50 Hz systems.

$$\begin{aligned} k_n &= 0.988 \\ \omega_{1n} &= 2\pi \cdot 1.37824 \\ \omega_{2n} &= 2\pi \cdot 0.00667 \\ \omega_{3n} &= 2\pi \cdot 0.03529 \\ \omega_{4n} &= 2\pi \cdot 0.11532 \end{aligned} \tag{12}$$

Deviations between both frequency characteristics regarding the amplitude are negligible, below 2.1% over the whole frequency range.

5. Comparison of both strategies

After the new linear system was designed, the final step was to compare the response of the new strategy with that of the IEC flickermeter. This comparison was performed under different analytical and real scenarios.

To carry out the comparison, a discrete implementation in Matlab of both specifications (IEC flickermeter, new strategy) for a 230 V/50 Hz system was performed. For both flickermeters, the input signal was processed at a sampling rate of $f_{\mathrm{s}} = 6400$ Hz. After the demodulation filters, the signal was decimated to reduce the sampling frequency to $f_{\mathrm{p}} = 800$ Hz. All the filters were implemented in the discrete domain by means of the bilinear transformation of the corresponding transfer function, using the proper sampling frequency for each filter, f_s or f_p. Both implementations do not include the high-pass demodulation filter of Block 3 as its main function is to remove the DC component and this goal is already achieved by means of the transmission zero of the weighting filter. For the IEC flickermeter, different techniques of classification are available to achieve accurate flicker evaluation over a wide range of conditions. In our implementation, the percentiles of P_inst were calculated for the complete set of samples, with the accuracy provided by Matlab. Moreover, the correct implementation and proper performance of the IEC flickermeter has been successfully tested in several previous works [8, 19].

5.1. Behavior under analytical experiments

The first comparison was based on the response to rectangular voltage changes from the $P_\mathrm{st} = 1$ curve. Different rectangular fluctuations were generated with modulating frequencies f_m up to 33.3 Hz and relative amplitude $\frac{\Delta V}{V}$ corresponding to the $P_\mathrm{st} = 1$ curve for each frequency. Note that the values of this curve have been used in this work to obtain the specification of the new linear system.

The relative amplitude values were obtained by means of the IEC flickermeter implementation as those values that produce $P_\mathrm{st} = 1$ with a maximum deviation of 10^{-5}. The fluctuations generated in this way were also processed using the new measurement strategy. Every flicker severity value was within the 1 ± 0.05 margin.

Judging by the problems detected in the behavior of the IEC flickermeter, a relevant comparison between the two strategies should consider nonuniform temporal fluctuation patterns. Fig. 2 shows the temporal fluctuation pattern used for this purpose. The input signal is composed of two segments: during a certain period t_ON there is a rectangular fluctuation of frequency f_ON and relative amplitude $A_\mathrm{ON} = \frac{\Delta V}{V}\big|_{P_\mathrm{st}=1}$; that is, the amplitude that would produce $P_\mathrm{st} = 1$ for the frequency f_ON if it were applied during the complete 10 min period. For the rest of the time up to 10 min, t_OFF, the fluctuation is deactivated.

Considering (2), this case is equivalent to a fluctuation applied during the whole 600 s period, of frequency f_{ON} and relative amplitude:

$$A_{\mathrm{eq}} = A_{\mathrm{ON}} \cdot \sqrt{\tfrac{t_{\mathrm{ON}}}{600}} \ . \tag{13}$$

Because the amplitude A_{ON} applied during 10 min produces $P_{\mathrm{st}} = 1$, the theoretical flicker severity value corresponding to the scheme of Fig. 2 is:

$$P_{\mathrm{st}}^{\mathrm{th}} = \sqrt{\tfrac{t_{\mathrm{ON}}}{600}} \ . \tag{14}$$

To simplify the comparison, the experiment was performed for a single frequency $f_{\mathrm{ON}} =$ 10 Hz. The activation time, t_{ON}, was increased from 0 to 600 s in 0.1 s steps. The resulting fluctuations were applied to both flickermeter implementations. The theoretical values, according to Ailleret's rules (14), were also calculated. Fig. 3 shows the results of the obtained flicker severity values in terms of the activation time, t_{ON}.

Analysis of Fig. 3 reveals several important conclusions. The P_{st}^{IEC} values provided by the IEC flickermeter show great deviation from the theoretical values, P_{st}^{th}. Additionally, it can be observed that the deviated P_{st}^{IEC} values rise abruptly and are distributed in 15 practically constant levels. This abnormal behavior is caused by the multipoint algorithm of Block 5 of the IEC flickermeter, based on the calculation of 15 different percentiles of P_{inst}. The procedure is as follows. For short activation times, t_{ON}, $P_{0.1}$ is the only percentile relevant for the algorithm. With increasing activation time, the effect of that percentile becomes gradually and slowly stronger. For a particular activation time, the next upper percentile becomes influential, generating an abrupt transition in flicker severity. The same effect applies to the rest of the percentiles. As demonstrated in [8], the multipoint algorithm provides accurate results when the rectangular fluctuation is applied uniformly during the whole period of 10 min. When the fluctuation is not applied in that manner, the evolution of the percentiles becomes unpredictable, and the P_{st}^{IEC} values depend heavily on the duration of the fluctuation, t_{ON}.

Otherwise, Fig. 3 shows that the P_{st}^{new} values provided by the new strategy fit with negligible deviations from the expected values. The new strategy considers the nonuniform characteristics of the fluctuations when using the RMS value for the flicker severity calculation, so it complies with the rule that correlates irritation and time (2).

5.2. Behavior under real scenarios

Assuming the complexity and irregularity of the real voltage signals, in this subsection the responses of the two strategies in real scenarios are compared. Different real voltage time series recorded at a site of the low voltage network in the North of Spain were used in the study. The site corresponded to a small town of 15.000 inhabitants located in a steel industry area in which arc furnaces are operating. The voltage time series were recorded at a rate of 6400 Hz and each record was processed through the digital implementations of both strategies, so that the corresponding P_{st} and P_{lt} values were obtained.

Fig. 4 depicts the time evolution of the P_{st} and P_{lt} values from both strategies. The selected short-term and long-term values were 10 min and 2 hours, respectively. The corresponding box-plots of each site are also represented, based on the cumulative probability function (CPF) of the P_{st} and P_{lt} sequences. The horizontal line of each box-plot represents the median of the distribution, and the bottom and top of the box indicate the 25 th and 75 th percentiles respectively, showing the dispersion of the distribution. Concentric circles have also been included to represent the minimum value and the 99 th percentile.

The box-plot shows that the periods of inactivity of the arc furnaces produced a dispersed distribution for the results provided by both strategies. The flicker severity values provided by the IEC flickermeter were significantly higher than those of the new strategy ($P_{lt}^{IEC} = 1.6$, $P_{lt}^{new} = 1.1$), mainly in time intervals during which the flicker levels were high. The irritability threshold was exceeded by 69% of the P_{lt}^{IEC} values and by only 9% of the P_{lt}^{new} values.

In brief, both strategies provided identical results when analyzing their response to the analytical fluctuations that define the $P_{st} = 1$ curve. However, under nonuniform voltage time series the results from both strategies were significantly different, both with analytical and real signals. The flicker severity values obtained with the new strategy were substantially lower than those obtained by the IEC flickermeter.

6. Conclusions

The manuscript presents an alternative strategy for flicker measurement that complies with the accuracy requirements established by the IEC 61000-4-15 standard. Moreover, this new strategy improves the response in the case of nonuniform fluctuations, which is more representative of real scenarios.

The current standard does not properly evaluate the real irritation produced by lights with nonuniform temporal fluctuation patterns because the current specification does not comply with Ailleret's time composition rule. The new strategy replaces the multipoint algorithm of Block 5 with a simple quadratic average. To achieve the accuracy required by the current standard, a new linear system needs to be inserted that adjusts the response of the meter for the whole frequency range.

This article provides the functional specifications of the new strategy, as well as the design of the new linear system; it also presents in detail the complex analytical process of obtaining the frequency specification of the new linear system. The accuracy of the new functional specification has been validated for digital implementation when subject to rectangular fluctuations corresponding to the flicker severity threshold. The comparison was also extended to a set of rectangular fluctuations characterized by a nonuniform temporal pattern and to real scenarios where an important level of irregularity of the voltage fluctuation is present.

Under nonuniform voltage time series the flicker severity values provided by the new strategy were substantially different from those of the IEC flickermeter. Although the IEC 61000-4-15 standard establishes that flicker measurement strategies need to be adjusted based on the standardized $P_{st} = 1$ curve, it is not acceptable that two strategies that meet this requirement do not provide similar values in real scenarios. Since the IEC flickermeter seems to overestimate the flickering sensation when compared with the new strategy, future works could investigate if this fact is the origin of the poor correlation between the flicker measurement and users' complaints.

To sum up, the new strategy has been designed considering the physiological behavior of the lamp–eye–brain set, just as it was for the current specification. Furthermore, it complies with the accuracy requirements established by the current standard, in relation to both the flicker perception, P_{inst}, and flicker severity, P_{st}. However, this new strategy also complies with the time composition rules, providing clear advantages when used in real scenarios. The implementation of the new strategy is simpler than the current one because it is based on the quadratic average for flicker severity calculation, avoiding the use of the multipoint algorithm and, hence, the classification process for the calculation of the CPF. This computational saving is an advantage for the new smart power quality meters that need to work on real-time [20]. The simplification involves two additional benefits: on the one hand, it allows us to delimit the implementation and to reduce the dispersion in results associated with the different techniques of the classification process; on the other hand, it provides a greater flexibility in selecting integration intervals different from those recommended by the current standard.

Acknowledgments

This work received financial support from the Government of the Basque Country through the PhD studentship BFI-2012-315 and from the University of the Basque Country UPV/EHU through the project UFI11/16 and the PhD studentship PIF 2011/169.

References

[1] C. Chen et al., An Accurate Solution Procedure for Calculation of Voltage Flicker Components, IEEE Trans. Ind. Electron. 61 (5) (2014) 2370–2377.

[2] Flicker Measurement and Evaluation, Tech. rep., UIE Disturbances WG (1992).

[3] IEC 61000-4-15 ED 2.0, Electromagnetic compatibility (EMC) Part 4: Testing and Measurement Techniques - Section 15: Flickermeter Functional and Design Specifications.

[4] D. Arlt et al., Examples of International Flicker Requirements in High Voltage Networks and Real World Measurements, in: Proc. of 9th EPQU, 2007, pp. 1–4.

[5] M. Halpin et al., Review of Flicker Objectives for HV, MV and LV Systems, CIGRE WG C4.108 (2009).

[6] C. Rong et al., Flicker Responses of Different Lamp Types, IET Gener. Transm. Dis. 3 (9) (2009) 816–824.

[7] M.L. Schenne et al., A Novel Adaptive Flicker Measurement Technique, Int. J. Electr. Power Energy Syst. 33 (10) (2011) 1686–1694.

[8] J. Ruiz et al., A Review of Flicker Severity Assessment by the IEC Flickermeter, IEEE Trans. Instrum. Meas 59 (8) (2010) 2037–2047.

[9] H. De Lange, Experiments on Flicker and some Calculations on an Electrical Analogue of the Foveal Systems, Physica 18 (11) (1952) 935–950.

[10] P. Ailleret, Détermination des Lois Expérimentales du Papillotement (Flicker) en vue de leur Application aux Réseaux Basse Tension sur lesquels les Charges Varient Périodiquement ou Aléatoirement (Soudeuses Démarrages de Moteurs), Bulletin de la Société Francaise des Electriciens 7 (77) (1957) 257–262.

[11] C. Rashbass, The Visibility of Transient Changes of Luminance, J. Physiol. 210 (1) (1970) 165–186.

[12] J. Koenderink, A. van Doorn, Visibility of Unpredictably Flickering Lights, J. Opt. Soc. Am 64 (11) (1974) 1517–1522.

[13] IEC. 555-3, Disturbances in Supply Systems Caused by Household Appliances and Similar Electric Equipment - Part 4: Voltage Fluctuations.

[14] M. Piekarz et al., Comparative Tests of Flickermeters, Proc. of 10th ICHQP (2002) 220–227.

[15] G. Wiczynski, Inaccuracy of Short-Term Light Flicker P-st Indicator Measuring with a Flickermeter, IEEE Trans. Power Del. 27 (2) (2012) 842–848.

[16] A. Hooshyar et al., Addressing IEC Flickermeter Deficiencies by Digital Filtration Inside a Sliding Window, IEEE Trans. Instrum. Meas. 62 (9) (2013) 2476–2491.

[17] Terms of Reference, Tech. rep., Review of LV and MV Compatibility Levels for Voltage Fluctuations, CIGRE WG C4.111 (2010).

[18] McKinsey & Company Inc., Lighting the way: Perspectives on the Global Lighting Market, `http://img.ledsmagazine.com/pdf/LightingtheWay.pdf`, [Online] (2011).

[19] J.J. Gutierrez et al., Effect of the Sampling Rate on the Assessment of Flicker Severity Due to Phase Jumps, IEEE Trans. Power Del. 26 (4) (2011) 2215–2222.

[20] R. K. M.K. Saini, Classification of Power Quality Events – A Review, Int. J. Electr. Power Energy Syst. 43 (1) (2012) 11–19.

Figure Captions

Figure 1	Block diagrams of the IEC flickermeter and the new strategy.
Figure 2	Layout of the nonuniform fluctuation.
Figure 3	Response to nonuniform temporal patterns.
Figure 4	P_{st} and P_{lt} values for the real voltage time series with the two strategies.

Figure 1

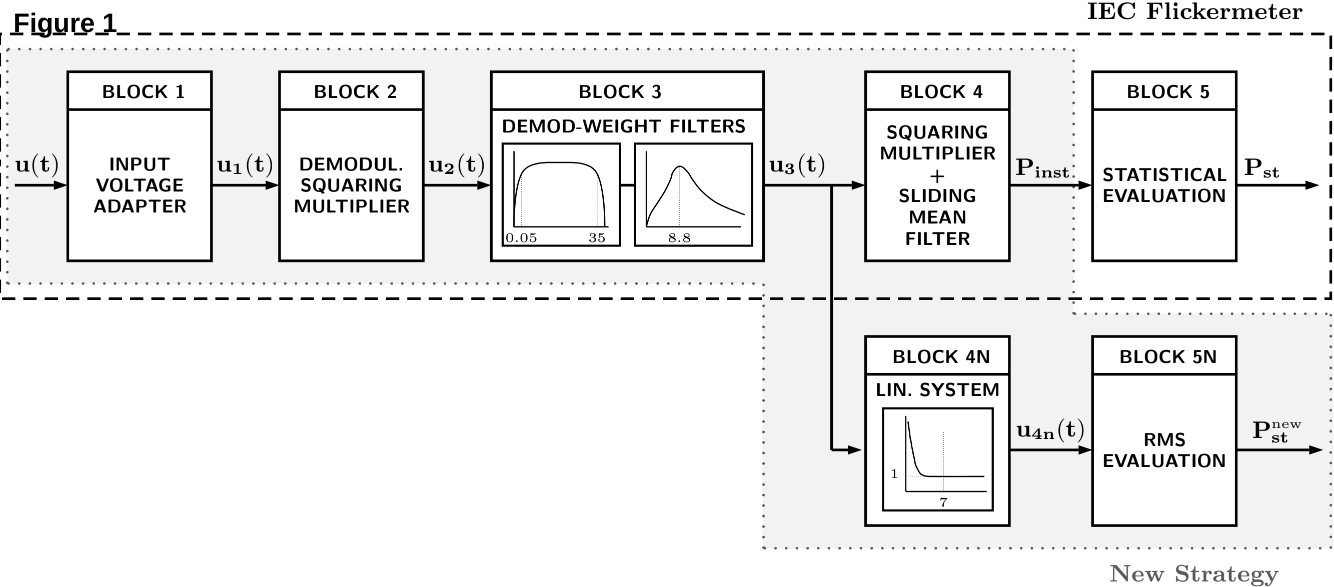

IEC Flickermeter
BLOCK 1
INPUT VOLTAGE ADAPTER
BLOCK 2
DEMODUL. SQUARING MULTIPLIER
BLOCK 3
DEMOD-WEIGHT FILTERS
0.05
35
8.8
BLOCK 4
SQUARING MULTIPLIER + SLIDING MEAN FILTER
BLOCK 5
STATISTICAL EVALUATION
u(t)
u1(t)
u2(t)
u3(t)
Pinst
Pst
BLOCK 4N
LIN. SYSTEM
1
7
u4n(t)
BLOCK 5N
RMS EVALUATION
Pst new
New Strategy

Figure 2

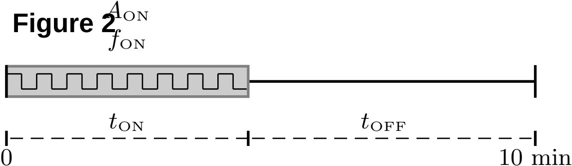

Figure 3

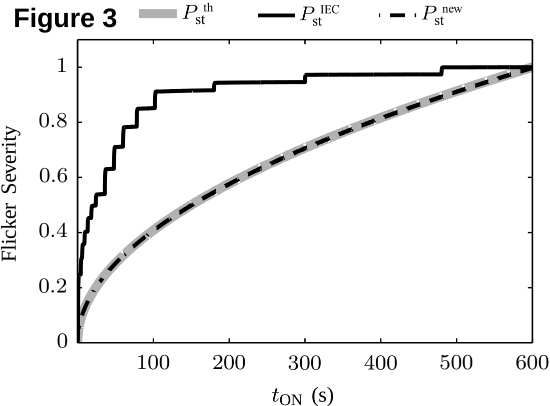

$P_{\mathrm{st}}^{\mathrm{th}}$
$P_{\mathrm{st}}^{\mathrm{IEC}}$
$P_{\mathrm{st}}^{\mathrm{new}}$
Flicker Severity
0
0.2
0.4
0.6
0.8
1
100
200
300
400
500
600
t_{ON} (s)

Figure 4

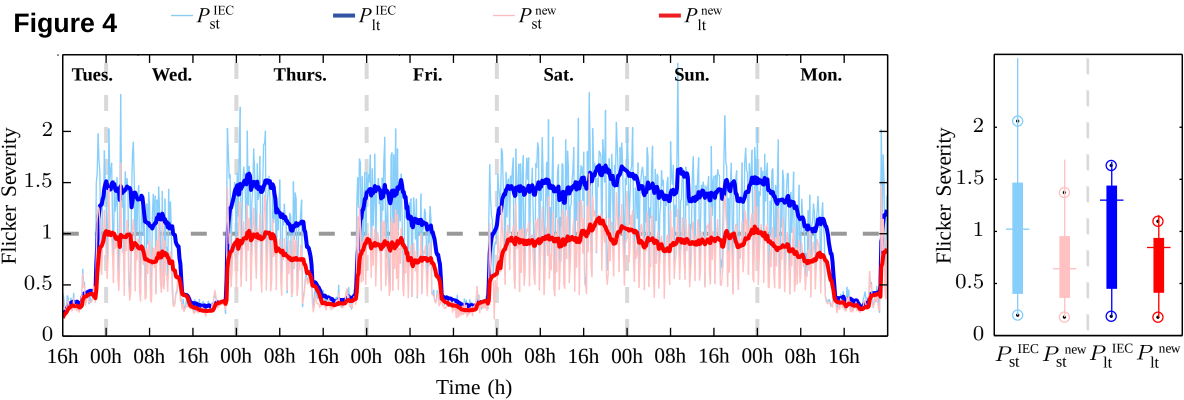

P_{st}^{IEC}
P_{lt}^{IEC}
P_{st}^{new}
P_{lt}^{new}
Tues.
Wed.
Thurs.
Fri.
Sat.
Sun.
Mon.
Flicker Severity
0
0.5
1
1.5
2
16h
00h
08h
16h
00h
08h
16h
00h
08h
16h
00h
08h
16h
00h
08h
16h
00h
08h
16h
Time (h)
Flicker Severity
0
0.5
1
1.5
2
P_{st}^{IEC}
P_{st}^{new}
P_{lt}^{IEC}
P_{lt}^{new}